JHEP

Published by Institute of Physics Publishing for SISSA

Received: *January 24, 2007*
Revised: *March 18, 2007*
Accepted: *March 25, 2007*
Published: *March 29, 2007*

# Hidden fermion as milli-charged dark matter in Stueckelberg $Z'$ model

**Kingman Cheung and Tzu-Chiang Yuan**

*Department of Physics, National Tsing Hua University, Hsinchu, Taiwan*
*Physics Division, National Center for Theoretical Sciences*
*Hsinchu, Taiwan*
*E-mail:* cheung@phys.nthu.edu.tw, tcyuan@phys.nthu.edu.tw

Abstract: We augment the hidden Stueckelberg $Z'$ model by a pair of Dirac fermions in the hidden sector, in which the $Z'$ has a coupling strength comparable to weak scale coupling. We show that this hidden fermion-antifermion pair could be a milli-charged dark matter candidate with a viable relic density. Existing terrestrial and astrophysical searches on milli-charged particles do not place severe constraints on this hidden fermion. We calculate the flux of monochromatic photons coming from the Galactic center due to pair annihilation of these milli-charged particles and show that it is within reach of the next generation $\gamma$-ray experiments. The characteristic signature of this theoretical endeavor is that the Stueckelberg $Z'$ boson has a large invisible width decaying into the hidden fermion-antifermion pair. We show that existing Drell-Yan data do not constrain this model yet. Various channels of singly production of this $Z'$ boson at the LHC and ILC are explored.

Keywords: Hadronic Colliders, Beyond Standard Model, LEP HERA and SLC Physics, Supersymmetric Standard Model.

JHEP03(2007)120

## Contents



JHEP03(2007)120

## 1. Introduction

The standard model (SM) of particle physics has been blessed with her elegant way of giving masses to the weak gauge bosons by the Higgs mechanism. However, the crucial ingredient of this mechanism, the Higgs boson, is still missing. In addition, a scalar Higgs boson mass is not stable under perturbative calculation. It will receive an enormous amount of radiative corrections to its mass such that a delicate cancellation between its bare mass and radiative corrections is needed so as to obtain a mass in the electroweak scale – this is the famous hierarchy problem. An alternative way to give mass to an abelian $U(1)$ gauge boson is known as the Stueckelberg mechanism. Although it is very difficult to give masses to nonabelian gauge bosons without sacrificing renormalizability within the Stueckelberg approach, it is worthwhile to study the consequence of this mechanism as an extension to the SM with extra abelian $U(1)$ factors.

Recently, Kors and Nath [1] showed that the SM extended by a hidden sector described by a Stueckelberg $U(1)_X$ and the gauge field $C_\mu$ associated with it can pass all the existing constraints from electroweak data as well as direct search limits from the Tevatron. Through the combined Stueckelberg and Higgs mechanisms, the SM $SU_L(2) \times U(1)_Y$ gauge fields $B_\mu$ and $W_\mu^3$ mix with the hidden sector gauge field $C_\mu$. After rotation from the interaction basis ($C_\mu$, $B_\mu$, $W_\mu^3$) to the mass eigenbasis ($Z'_\mu, Z_\mu, A_\mu$), one obtains a massless state identified to be the photon $\gamma$ and two massive eigenstates which are the SM-like $Z$

boson and an additional $Z'$ boson. As long as the mixing is small, the $Z'$ boson only couples very weakly to the SM fermions, and so it can evade all the existing constraints on conventional $Z'$ models. The allowed mass range for the Stueckelberg $Z'$ can be anywhere from 200 GeV to a few TeV [2]. Typically, the mass of the Stueckelberg $Z'$ is above the SM $Z$ boson mass.

In this work, a pair of hidden Dirac fermions is introduced in the Stueckelberg $Z'$ model. Such a possibility has been mentioned in ref. [1], but its phenomenology was not explored. There could be various types or generations of fermions in the hidden sector, just like our visible world. Since the abelian $U(1)_X$ is assumed to be the only gauge group in the hidden sector and there is no connector sector between our visible world and the hidden one in this class of models, all hidden fermions in this sector are stable. [1] Thus the hidden fermion-antifermion pair that we add in the model can be viewed as the lightest ones in the hidden sector, should there be more than one type of them. The SM fermions are neutral under this hidden $U(1)_X$. Since this hidden fermion pair is stable, it can be the dark matter candidate of our Universe.

In the next section, we will present some details of the Stueckelberg $Z'$ extension of the SM with an additional pair of Dirac fermion-antifermion in the hidden sector. In section III, we discuss milli-charged dark matter. Treating the hidden fermion as our candidate of dark matter, we calculate its relic density and explore the parameter space allowed by the WMAP measurement. We also calculate the monochromatic photon flux coming from the Galactic center due to pair annihilation of these hidden fermions. In section IV, we explore some novel collider phenomenology of the Stueckelberg $Z'$ with the presence of the hidden fermion. Since the width of the Stueckelberg $Z'$ is no longer narrow, compared to the scenario studied in [2], its phenomenology is rather different. Comments and conclusions are given in section V.

## 2. The model

The Stueckelberg extension [1] of the SM (StSM) is obtained by adding a hidden sector associated with an extra $U(1)_X$ interaction, under which the SM particles are neutral. [2] We explicitly specify the content of the hidden sector: a gauge boson $C_\mu$ and a pair of fermion and antifermion $\chi$ and $\bar{\chi}$.

The Lagrangian describing the system is $\mathcal{L}_{\rm StSM} = \mathcal{L}_{\rm SM} + \mathcal{L}_{\rm St}$, where

$$\begin{aligned}\mathcal{L}_{\rm SM} =& -\frac{1}{4}W^a_{\mu\nu}\,W^{a\mu\nu} - \frac{1}{4}B_{\mu\nu}\,B^{\mu\nu} + D_\mu\Phi^\dagger\,D^\mu\Phi - V(\Phi^\dagger\,\Phi) \\ &+ i\bar{\psi}_f\gamma^\mu D_\mu\psi_f\ , \qquad (2.1)\\ \mathcal{L}_{\rm St} =& -\frac{1}{4}C_{\mu\nu}\,C^{\mu\nu} + i\bar{\chi}\gamma^\mu D^X_\mu\chi - \frac{1}{2}\left(\partial_\mu\sigma + M_1C_\mu + M_2B_\mu\right)^2\ , \qquad (2.2)\\ D_\mu =& \partial_\mu + ig_2\frac{\tau^a}{2}\,W^a_\mu + ig_Y\frac{Y}{2}B_\mu\ , \qquad (2.3)\end{aligned}$$

[1] This is in analogous to the pure QED case, muon does not decay into an electron plus a photon.

[2] It was shown in ref. [1] that the SM fermions are neutral under the extra $U(1)_X$ has the advantage of maintaining the neutron charge to be zero.



JHEP03(2007)120

$$D_\mu^X = \partial_\mu + i g_X Q_X C_\mu \,, \tag{2.4}$$

where $W^a_{\mu\nu}(a = 1, 2, 3)$, $B_{\mu\nu}$, and $C_{\mu\nu}$ are the field strength tensors of the gauge fields $W^a_\mu$, $B_\mu$, and $C_\mu$, respectively. The SM fermions $f$ were explicitly forbidden from carrying the $U(1)_X$ charges, as implied by eq. (2.3), while the hidden fermion pair only carries the $U(1)_X$ charge, as implied by eq. (2.4). One can show that the scalar field $\sigma$ decouples from the theory after gauge fixing terms are added upon quantization.

The mass term for $V \equiv (C_\mu,\, B_\mu,\, W^3_\mu)^T$, after electroweak symmetry breaking $\langle\Phi\rangle = v/\sqrt{2}$, is given by [1]

$$-\frac{1}{2}V^T M V \equiv -\frac{1}{2}\left(C_\mu,\, B_\mu,\, W^3_\mu\right) \begin{pmatrix} M_1^2 & M_1 M_2 & 0 \\ M_1 M_2 & M_2^2 + \frac{1}{4}g_Y^2 v^2 & -\frac{1}{4}g_2 g_Y v^2 \\ 0 & -\frac{1}{4}g_2 g_Y v^2 & \frac{1}{4}g_2^2 v^2 \end{pmatrix} \begin{pmatrix} C_\mu \\ B_\mu \\ W^3_\mu \end{pmatrix} . \tag{2.5}$$

A similarity transformation can bring the mass matrix $M$ into a diagonal form

$$\begin{pmatrix} C_\mu \\ B_\mu \\ W^3_\mu \end{pmatrix} = O \begin{pmatrix} Z'_\mu \\ Z_\mu \\ A_\mu \end{pmatrix} \quad , \qquad O^T M\, O = \mathrm{diag}(m^2_{Z'},\, m^2_Z,\, 0) \,. \tag{2.6}$$

The $m^2_{Z'}$ and $m^2_Z$ are given by

$$\begin{aligned} m^2_{Z',\,Z} = \frac{1}{2}\Bigg[ & M_1^2 + M_2^2 + \frac{1}{4}(g_Y^2 + g_2^2)v^2 \\ & \pm\sqrt{(M_1^2 + M_2^2 + \frac{1}{4}g_Y^2 v^2 + \frac{1}{4}g_2^2 v^2)^2 - (M_1^2(g_Y^2 + g_2^2)v^2 + g_2^2 M_2^2 v^2)}\Bigg] \,. \end{aligned} \tag{2.7}$$

The orthogonal matrix $O$ is parameterized as [3]

$$O = \begin{pmatrix} c_\psi c_\phi - s_\theta s_\phi s_\psi & s_\psi c_\phi + s_\theta s_\phi c_\psi & -c_\theta s_\phi \\ c_\psi s_\phi + s_\theta c_\phi s_\psi & s_\psi s_\phi - s_\theta c_\phi c_\psi & c_\theta c_\phi \\ -c_\theta s_\psi & c_\theta c_\psi & s_\theta \end{pmatrix} , \tag{2.8}$$

where $s_\phi = \sin\phi, c_\phi = \cos\phi$ and similarly for the angles $\psi$ and $\theta$. The angles are related to the original parameters in the Lagrangian $\mathcal{L}_{\mathrm{StSM}}$ by

$$\delta \equiv \tan\phi = \frac{M_2}{M_1}, \;\; \tan\theta = \frac{g_Y \cos\phi}{g_2}, \;\; \tan\psi = \frac{\tan\theta\, \tan\phi\, m_W^2}{\cos\theta[m^2_{Z'} - m_W^2(1 + \tan^2\theta)]} \,, \tag{2.9}$$

where $m_W = g_2 v/2$. The Stueckelberg $Z'$ decouples from the SM when $\phi \to 0$, since

$$\tan\phi = \frac{M_2}{M_1} \to 0 \;\; \Rightarrow \;\; \tan\psi \to 0 \;\; \text{and} \;\; \tan\theta \to \tan\theta_{\mathrm{w}}$$

where $\theta_{\mathrm{w}}$ is the Weinberg angle.

[3] We note that the middle column is chosen to be different from that of ref. [1] by an overall minus sign.

The interactions of fermions with the neutral gauge bosons before rotating to the mass eigenbasis are given by

$$-\mathcal{L}_{\rm int}^{NC} = g_2 W_\mu^3 \,\bar\psi_f \gamma^\mu \frac{\tau^3}{2}\psi_f + g_Y B_\mu \,\bar\psi_f \gamma^\mu \frac{Y}{2}\psi_f + g_X C_\mu \,\bar\chi \gamma^\mu Q_X \chi \,, \tag{2.10}$$

where $f$ denotes the SM fermions. The neutral gauge fields are rotated into the mass eigenbasis using eq. (2.8), and the above neutral current interaction becomes

$$\begin{aligned} -\mathcal{L}_{\rm int}^{NC} &= \bar\psi_f \,\gamma^\mu \left[\left(\epsilon_{Z'}^{f_L} P_L + \epsilon_{Z'}^{f_R} P_R\right) Z'_\mu + \left(\epsilon_Z^{f_L} P_L + \epsilon_Z^{f_R} P_R\right) Z_\mu + e Q_{\rm em} A_\mu\right] \psi_f \\ &\quad + \bar\chi \gamma^\mu \left[\epsilon_\gamma^\chi A_\mu + \epsilon_Z^\chi Z_\mu + \epsilon_{Z'}^\chi Z'_\mu\right] \chi \,, \end{aligned} \tag{2.11}$$

where

$$\begin{aligned} \epsilon_\gamma^\chi &= g_X Q_X^\chi (-c_\theta s_\phi) \,, \\ \epsilon_Z^\chi &= g_X Q_X^\chi (s_\psi c_\phi + s_\theta s_\phi c_\psi) \,, \\ \epsilon_{Z'}^\chi &= g_X Q_X^\chi (c_\psi c_\phi - s_\theta s_\phi s_\psi) \,, \\ \epsilon_Z^{f_{L,R}} &= \frac{c_\psi}{\sqrt{g_2^2 + g_Y^2 c_\phi^2}} \left(-c_\phi^2 g_Y^2 \frac{Y}{2} + g_2^2 \frac{\tau}{2}\right) + s_\psi s_\phi g_Y \frac{Y}{2} \,, \\ \epsilon_{Z'}^{f_{L,R}} &= \frac{s_\psi}{\sqrt{g_2^2 + g_Y^2 c_\phi^2}} \left(c_\phi^2 g_Y^2 \frac{Y}{2} - g_2^2 \frac{\tau}{2}\right) + c_\psi s_\phi g_Y \frac{Y}{2} \,. \end{aligned} \tag{2.12}$$

In the above, we have used the relations

$$e = g_2 \, s_\theta = g_Y c_\phi c_\theta \qquad \text{and} \qquad Q_{\rm em} = \frac{\tau^3}{2} + \frac{Y}{2} \,,$$

where $Q_{\rm em}$ is the electric charge operator. From eqs. (2.11)–(2.12), it is clear that in this class of model, the SM fermions interact with the hidden world through $Z'$ and the hidden fermion interacts with our visible world through $\gamma$ and $Z$. In our computation, we assume the following input parameters at the electroweak scale [3]

$$\alpha_{\rm em}(m_Z) = \frac{1}{128.91}, \;\; G_F = 1.16637 \times 10^{-5}\,{\rm GeV}^{-2}, \;\; m_Z = 91.1876\,{\rm GeV} \,, \sin^2\theta_{\rm w} = 0.231 \,,$$

and the following three inputs related to the hidden sector

$$\delta \equiv \tan\phi, \;\; g_X, \;\; \text{and} \;\; M_{Z'} \,.$$

Since $Q_X^\chi$ always enters in the product form $g_X Q_X^\chi$, one can set $Q_X^\chi$ to be unity without loss of generality. We derive from $\alpha_{\rm em}$, $G_F$, $m_Z$, and $\sin^2\theta_{\rm w}$ the values of

$$e = \sqrt{4\pi\alpha_{\rm em}} \,, \; v = \left(\sqrt{2} G_F\right)^{-1/2} \,, \; m_W = m_Z \sqrt{1 - \sin^2\theta_{\rm w}} \,, \;\; \text{and} \;\; g_2 = 2 m_W / v \,.$$

We then fix the value of $g_Y$ by the following equation

$$e = \frac{g_2 g_Y c_\phi}{\sqrt{g_2^2 + g_Y^2 c_\phi^2}} \,.$$

The other two angles $\theta$ and $\psi$ are determined from the last two formulas in eq. (2.9).

It is clear from eqs. (2.11)-(2.12) that the chiral couplings of the SM $Z$ boson are affected by the mixing. In fact, even the mass of the $Z$ boson is modified in this model, as shown by eq. (2.7). It has been shown in ref. [2] that in order to keep the $Z$ boson mass within the experimental uncertainty, the mixing angle must satisfies

$$\delta \lesssim 0.061 \sqrt{1 - (m_Z/M_1)^2} \, . \tag{2.13}$$

When $\delta$ is small and $m_{Z'}$ is large, $M_1 \approx m_{Z'} + O(g_2 v)$. The constraint coming from the electroweak precision data is more or less the same as in eq. (2.13) [2].

The limits obtained in ref. [2] also included the analysis from direct $Z'$ production at the Tevatron. They showed that with the current Drell-Yan data,

$$\begin{aligned} m_{Z'} &> 250 \text{ GeV} \quad \text{for} \quad \delta \approx 0.035 \, , \\ m_{Z'} &> 375 \text{ GeV} \quad \text{for} \quad \delta \approx 0.06 \, . \end{aligned} \tag{2.14}$$

If including the presence of a hidden fermion that the Stueckelberg $Z'$ can couple to, the limit from direct $Z'$ direction would be relaxed because of the smaller production rate into visible lepton pairs [2]. In section IV, we will show that with a hidden fermion $\chi$ fulfilling the dark matter constraint, the $Z'$ would dominantly decay into the hidden sector fermion pair provided that $m_{Z'} > 2m_\chi$. It would therefore entirely remove the constraint in eq. (2.14) from direct production. On the other hand, if $m_{Z'} < 2m_\chi$ the $Z'$ boson cannot decay into the hidden sector fermions, and so the constraint in eq. (2.14) stands.

In the following numerical works, we will apply the constraints on $\delta$ and $m_{Z'}$ given by eqs. (2.13) and (2.14) respectively, but when $m_{Z'} > 2m_\chi$ the latter constraint will be dropped.

## 3. Dark matter phenomenology

### 3.1 Milli-charged dark matter

Milli-charged dark matter was first discussed by Goldberg and Hall [4], motivated by the work of Holdom [5] in which milli-charged particles in the hidden sector can interact with the visible photon due to kinetic mixing between the visible photon and the hidden or shadow photon. Numerous constraints for the milli-charged particles, including accelerator experiments, invisible decay in ortho-positronium, SLAC milli-charged particle search, Lamb shift, big-bang nucleosynthesis, dark matter search, search of fractional charged particles in cosmic rays, and other astrophysical reactions, were summarized in [6] (see figure 1 of the first reference in [6]). Study of the constraints on milli-charged particles from neutron stars and CMB measurements were discussed in refs. [7] and [8] respectively. In summary, milli-charged particles of mass from MeV to TeV with a fractional electric charge $(10^{-6} - 10^{-1})$ of a unit charge are still allowed. We note that integral charged dark matter was contemplated in [9] and composite dark matter was studied in [10]. More recently, PVLAS [11] reported a positive signal of vacuum magnetic dichroism. It has been suggested [12] that photon-initiated pair production of milli-charged fermions with a mass



JHEP03(2007)120

range between 0.1 to a few eV and a milli-charge $O(10^{-6})$ of a unit charge can explain the signal. However, this signal has not been confirmed by other experiments like the Q & A experiment [13]. For detailed analysis of various experiments of vacuum magnetic dichroism, we refer our readers to ref. [14].

### 3.2 Relic density and WMAP measurement

The first set of processes we consider in our relic density calculation are

$$\chi\bar{\chi} \to Z', Z, \gamma \to f\bar{f}$$

where $f$ is any SM fermion. The amplitude for the annihilation $\chi(p_1)\ \bar{\chi}(p_2) \to f(q_1)\ \bar{f}(q_2)$ can be written as

$$\mathcal{M} = \bar{v}(p_2)\,\gamma_\mu\,u(p_1) \times \bar{u}(q_1)\,\gamma^\mu\ (\xi_L P_L + \xi_R P_R)\ v(q_2) \tag{3.1}$$

where $P_{L,R} = (1 \mp \gamma_5)/2$, and

$$\xi_{L,R} = \frac{\epsilon_\gamma^\chi e Q_{\rm em}^f}{s} + \frac{\epsilon_Z^\chi \epsilon_Z^{f_{L,R}}}{s - m_Z^2} + \frac{\epsilon_{Z'}^\chi \epsilon_{Z'}^{f_{L,R}}}{s - m_{Z'}^2}\,. \tag{3.2}$$

The differential cross section is given by

$$\frac{d\sigma}{dz} = \frac{N_f}{32\pi}\,\frac{\beta_f}{s\beta_\chi}\left[(\xi_L^2 + \xi_R^2)(u_m^2 + t_m^2 + 2m_\chi^2(s - 2m_f^2)) + 4\,m_f^2\,\xi_L\xi_R(s + 2m_\chi^2)\right] \tag{3.3}$$

where $\beta_{f,\chi} = (1 - 4m_{f,\chi}^2/s)^{1/2}$, $N_f = 3\,(1)$ for $f$ being a quark (lepton), $t_m = t - m_\chi^2 - m_f^2 = -s(1 - \beta_f\beta_\chi z)/2$, $u_m = u - m_\chi^2 - m_f^2 = -s(1 + \beta_f\beta_\chi z)/2$, $s$ is the square of the center-of-mass energy, and $z \equiv \cos\Theta$ with $\Theta$ the scattering angle.

We also consider pair annihilation of $\chi\bar{\chi}$ into two neutral gauge bosons,

$$\chi\bar{\chi} \to V_1 V_2 \quad \text{with} \quad V_{1,2} = \gamma,\ Z,\ Z' \tag{3.4}$$

in our relic density calculation [4]. The differential cross section is given by

$$\begin{aligned}\frac{d\sigma(\chi\bar{\chi} \to V_1V_2)}{d\Omega} = \frac{S(\epsilon_{V_1}^\chi)^2(\epsilon_{V_2}^\chi)^2\beta_{V_1V_2}}{64\pi^2 s\beta_\chi}\Bigg\{ &-2\left(2\,m_\chi^2 + m_{V_1}^2\right)\left(2\,m_\chi^2 + m_{V_2}^2\right)\left(\frac{1}{u_\chi^2} + \frac{1}{t_\chi^2}\right) \\ &+ 2\left(\frac{t_\chi}{u_\chi} + \frac{u_\chi}{t_\chi}\right) - 4\left(\frac{1}{u_\chi} + \frac{1}{t_\chi}\right)\left(2\,m_\chi^2 + m_{V_1}^2 + m_{V_2}^2\right) \\ &- \frac{4}{u_\chi t_\chi}\left(2\,m_\chi^2 + m_{V_1}^2 + m_{V_2}^2\right)\left(2\,m_\chi^2 - m_{V_1}^2 - m_{V_2}^2\right)\Bigg\}\theta(2m_\chi - m_{V_1} - m_{V_2})\end{aligned} \tag{3.5}$$

where $\beta_{V_1V_2} = \lambda^{1/2}\left(1, m_{V_1}^2/s,\, m_{V_2}^2/s\right)$ with $\lambda(a,b,c) = a^2 + b^2 + c^2 - 2(ab + bc + ca)$ is the Mandelstam function, $t_\chi$ and $u_\chi$ are given by $t_\chi = t - m_\chi^2$ and $u_\chi = u - m_\chi^2$ respectively, and $S$ is the statistical factor. We note that processes $\chi\bar{\chi} \to \gamma\gamma, ZZ$ are doubly suppressed

[4] We have ignored the channel $\chi\bar{\chi} \to \gamma, Z, Z' \to W^+W^-$ which may contribute to certain extent.

by the small mixing angles and $\chi\bar{\chi} \to Z'Z'$ are either suppressed or forbidden by phase space, and therefore their contributions are negligible in the annihilation rates.

The quantity that is relevant in the relic density calculation is the thermal averaged cross section $\langle\sigma v\rangle$, where $v$ is the relative velocity of two annihilating particles. In the non-relativistic approximation, $v \simeq 2\,\beta_\chi$. To estimate the relic density of a weakly-interacting massive particle, we use the following formula [15]

$$\Omega_\chi h^2 \simeq \frac{0.1 \text{ pb}}{\langle\sigma v\rangle} .$$

With the most recent WMAP [16] result on dark matter density

$$\Omega_{\rm CDM} h^2 = 0.105 \pm 0.009 ,$$

where we have used the WMAP-data-only fit and taken $\Omega_{\rm CDM} = \Omega_{\rm matter} - \Omega_{\rm baryon}$, one can translate this WMAP data into

$$\langle\sigma v\rangle \simeq 0.95 \pm 0.08 \text{ pb} . \tag{3.6}$$

In estimating the annihilation rate during the freeze-out, we assume that the species has a velocity-squared $v^2 \simeq 0.1$. To get a crude estimation, we ignore the thermal average and evaluate $\sigma v$ directly.

In figure 1(a) and (b), we show the contours of $\sigma v = 0.95 \pm 0.16$ pb ($2\,\sigma$ range) in the plane of ($g_X$, $\delta$) for various input values of $m_{Z'}$ and $m_\chi$. We have included $\chi\bar{\chi} \to \gamma Z', ZZ'$, and $f\bar{f}$, with $f = \nu_e$, $\nu_\mu$, $\nu_\tau$, $e^-$, $\mu^-$, $\tau^-$, $u$, $d$, $s$, $c$, $b$, and $t$ that are kinematically allowed. From figure1(a) for $m_\chi = 60$ GeV and $m_{Z'} = 300$ GeV, we can see that $\delta \simeq 0.03$ and $g_X \simeq 0.6$ can give the correct amount of dark matter. Similarly, from figure1(b) with the same $m_\chi = 60$ GeV and a larger $m_{Z'} = 600$ GeV, $\delta \simeq 0.03$ and a slightly larger $g_X \simeq 0.7$ can also do the job. For comparison, we note that $e \simeq 0.31$ and $g_2 \simeq 0.65$ in the SM. Thus, the value of the hidden $U_X(1)$ coupling $g_X$ that we deduced from the WMAP measurement has the same order of the weak coupling $g_2$ of the visible sector. In figure 1(c), we show the annihilation rate $\sigma v$ versus $m_\chi$ for $\delta = 0.03$, $g_X = g_2$, and a fixed $m_{Z'} = 500$ GeV. Clear resonance structures of $Z$ and $Z'$ are seen. In figure 1(d), we show the contours of $\sigma v$ in the $(m_\chi, m_{Z'})$ plane. There are two branches: (i) the upper branch where $m_\chi < m_{Z'}/2$ and the band relating $m_\chi$ and $m_{Z'}$ is relatively wide; (ii) the lower branch where $2m_\chi > m_{Z'}$ and the band relating $m_\chi$ and $m_{Z'}$ is quite narrow. A narrow band implies the need of a fine-tuned relation between $m_\chi$ and $m_{Z'}$ in order to give the correct dark matter density. In the latter branch, the Tevatron bound of $m_{Z'} > 250$ GeV for $\delta \approx 0.03$ has to be imposed. Therefore, the case of $m_\chi < m_{Z'}/2$ is more preferred theoretically.

The hidden fermion $\chi$ couples to the photon via the mixing angles $c_\theta s_\phi$, the value of which is about $0.9 \times 0.03 \approx 0.03$. Therefore, effectively the fermion $\chi$ "acquires" an electric charge of $g_X Q_X^\chi c_\theta s_\phi / e \approx 0.06$, when its coupling to the photon is considered. Therefore, the range of $m_\chi \sim O(100)$ GeV and the size of effective electric charge $\simeq 0.06$ implied by dark matter density requirement in our calculation are consistent with the constraints on milli-charged particles [6].



JHEP03(2007)120

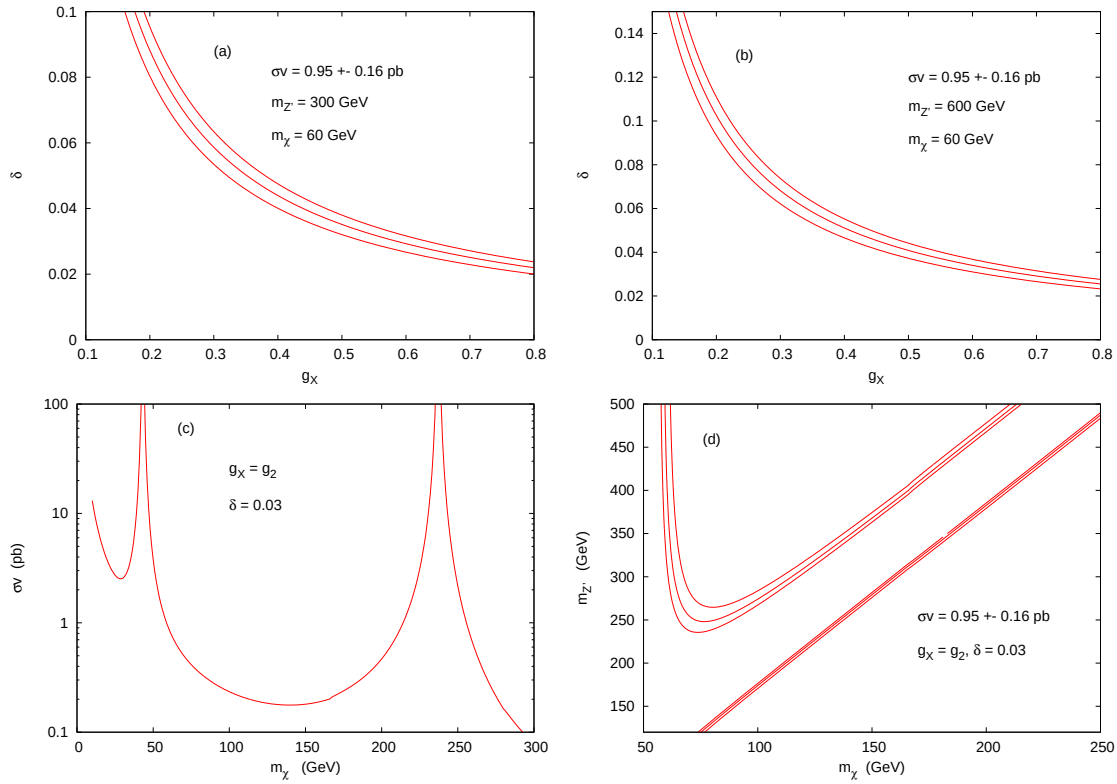


**Figure 1:** (a)–(b) are contours of $\sigma v = 0.95 \pm 0.16$ pb (2 $\sigma$ range) in the plane of $(g_X, \delta)$ for various $m_{Z'}$ and $m_\chi$. Part (c) shows the annihilation rate $\sigma v$ versus $m_\chi$ with $m_{Z'} = 500$ GeV, $g_X = g_2$, and $\delta = 0.03$. Part (d) shows the contour of $\sigma v = 0.95 \pm 0.16$ pb (2 $\sigma$ range) in the $(m_\chi, m_{Z'})$ plane.

### 3.3 Indirect detection

If milli-charged hidden fermions like $\chi$ and $\bar{\chi}$ are the dark matter, their pair annihilation into $\gamma\gamma, \gamma Z$, and $\gamma Z'$ in regions of high dark matter density, e.g. the Galactic center, can give rise to monochromatic $\gamma$-ray line that can reach our Earth for their indirect detection. The cross sections for these processes can be obtained from eq. (3.5) readily. The observed $\gamma$-ray flux along the line-of-sight between the Earth and the Galactic center is given by [15]

$$\Phi_\gamma(\psi, E) = \sigma v \frac{dN_\gamma}{dE_\gamma} \frac{1}{4\pi m_\chi^2} \int_{\text{line of sight}} ds \rho^2(r(s,\psi)) \ , \tag{3.7}$$

where the coordinate $s$ runs along the line of sight in a direction making an angle $\psi$ from the direction of the Galactic center, $dN_\gamma/dE_\gamma$ is the energy spectrum of the $\gamma$-rays, and $v \approx 2\beta_\chi$ is the relative velocity of the dark matter $\chi$ and $\bar{\chi}$, and the present value of $v \approx 10^{-3}$. The flux from a solid angle $\Delta\Omega$ is often expressed as

$$\Phi_\gamma(\Delta\Omega, E) \approx 5.6 \times 10^{-12} \frac{dN_\gamma}{dE_\gamma} \left(\frac{\sigma v}{\text{pb}}\right) \left(\frac{1\,\text{TeV}}{m_\chi}\right)^2 \overline{J}(\Delta\Omega) \Delta\Omega \, \text{cm}^{-2}\,\text{s}^{-1} \ , \tag{3.8}$$



JHEP03(2007)120

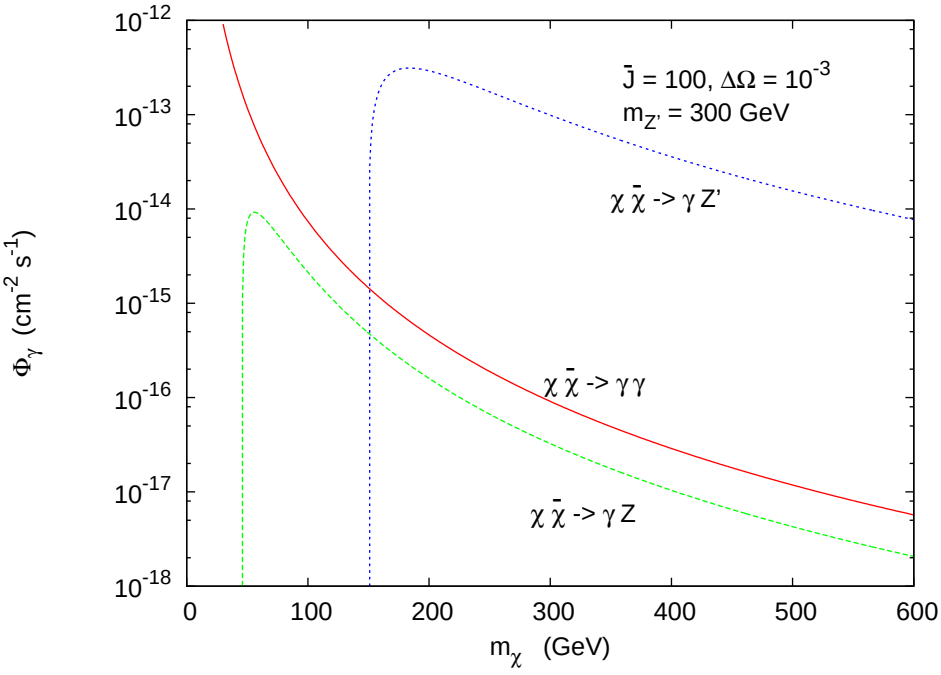


**Figure 2:** The resulting photon flux from annihilation processes $\chi\bar{\chi} \to \gamma\gamma$, $\gamma Z$, and $\gamma Z'$. We have used typical values of $\overline{J} = 100$, $\Delta\Omega = 10^{-3}$, and the present value of $v \approx 10^{-3}$.

with the quantity $J(\psi)$ defined by

$$J(\psi) = \frac{1}{8.5\,\mathrm{kpc}} \left( \frac{1}{0.3\,\mathrm{GeV/cm^3}} \right)^2 \int_{\text{line of sight}} ds \rho^2(r(s,\psi)) \; . \tag{3.9}$$

For the process of $\chi\bar{\chi} \to \gamma\gamma$, we would have a mono-energetic $\gamma$-ray line with $dN_\gamma/dE_\gamma \approx 2\delta(E_\gamma - m_\chi)$. Such a line, if observed, would be a distinctive signal for dark matter annihilation. Similarly, processes $\chi\bar{\chi} \to \gamma Z$ and $\chi\bar{\chi} \to \gamma Z'$ will have a photon energy spectrum as $dN_\gamma/dE_\gamma \approx \delta(E_\gamma - m_\chi(1 - m_{Z,Z'}^2/4m_\chi^2))$. The contributions from these processes to the photon flux are shown in figure 2 with $\overline{J} = 100$ and $\Delta\Omega = 10^{-3}$. In this plot, we have taken a moderate value for $\overline{J} = 100$ (averaged over $10^{-3}$ sr at the Galactic center). From table 7 of ref. [15], we know the value of $\overline{J}$ varies from $2.166 \times 10$ (Kra profile) to $1.352 \times 10^3$ (NFW profile) and to $1.544 \times 10^5$ (Moore profile). There are also cold dark matter profiles with dense spikes [17] near the Galactic center due to the accretion by central black holes that can give rise significant enhancement to the quantity $\overline{J}$. With a rather conservative choice of $\overline{J} = 100$, the flux of the $\gamma$-rays from the process $\chi\bar{\chi} \to \gamma\gamma$ is quite small due to double suppression of $(\epsilon_\gamma^\chi)^2$. The process $\chi\bar{\chi} \to \gamma Z$ contributes at a somewhat lower flux level. The process $\chi\bar{\chi} \to \gamma Z'$ can also contribute to the monochromatic photon flux, provided that $2m_\chi > m_{Z'}$. Since this process is only suppressed by one power of the mixing angle, it could be more substantial than the doubly-suppressed process $\chi\bar{\chi} \to \gamma\gamma$. Note that since $2m_\chi > m_{Z'}$, the Tevatron bound eq. (2.14) of $m_{Z'} > 250$ GeV for $\delta \approx 0.035$ must be enforced. When kinematics allowed, the photon flux from this process is three orders of magnitude higher than that from $\chi\bar{\chi} \to \gamma\gamma$. For comparison, we note that the



JHEP03(2007)120

photon flux from the neutralino pair annihilation $\tilde{\chi}^0\tilde{\chi}^0 \to \gamma\gamma$ [18] has been estimated to be about $1.5 \times 10^{-14}$ ($2 \times 10^{-13}$) cm$^{-2}$s$^{-1}$ if the neutralino is a Higgsino-LSP (Wino-LSP), using the same moderate value of $\overline{J} = 100$ [19, 20].

The expected sensitivities for the new Atmospheric Cerenkov Telescope (ACT) experiments such as HESS [21] and VERITAS [22] are at the level of $(10^{-14} - 10^{-13})$ cm$^{-2}$ s$^{-1}$ with an angular coverage of about $10^{-3}$. They are sensitive to the $\gamma$-rays from a few hundred GeV to TeV. On the other hand, the Gamma-ray Large Area Space Telescope (GLAST) experiment [23] due for launch in Fall this year, can probe $\gamma$-rays from 20 MeV to 300 GeV, but at a lower sensitivity level about $2 \times 10^{-9} - 10^{-10}$ cm$^{-2}$ s$^{-1}$. From figure 2, there is a small range of $m_\chi$ ( $m_\chi < 100$ GeV) such that $\chi\bar{\chi} \to \gamma\gamma$ contributes at a level larger than $10^{-14}$ cm$^{-2}$ s$^{-1}$. The process $\chi\bar{\chi} \to \gamma Z$ contributes at a level below the sensitivities of all these experiments for all ranges of $m_\chi$, whereas the process $\chi\bar{\chi} \to \gamma Z'$ can contribute at a much larger flux and it is indeed above the sensitivity level of ACT experiments for $m_\chi < 600$ GeV. Since GLAST can only be sensitive to $\gamma$-rays of 300 GeV or less with lower sensitivity, it is hard to detect the $\gamma$-rays from the lighter milli-charged dark matter. For heavier milli-charged dark matter, the $\gamma$-rays can be above a few hundred GeV and thus above the sensitivity reaches of HESS and VERITAS.

The continuum $\gamma$-ray background from astrophysical sources near Galactic Center is largely an unsettled issue due to astrophysical uncertainties. There have been data showing excess of $\gamma$-rays in different energy regimes near the Galactic center. The EGRET experiment [24] has reported an excess of $\gamma$-rays in the region of the Galactic center, including the galactic longitude and latitude position at $l = 0^\circ$ and $b = 0^\circ$ degrees. The level of excess is above the expectation of primary cosmic rays interacting with interstellar medium. The EGRET excess region is around 1 GeV. However, there may be some other unknown sources of $\gamma$-rays around the Galactic center. It is hard to establish the fact that the excess is due to dark matter annihilation, because the excess does not have specific features. This is in contrast to the monochromatic $\gamma$-ray flux, which is a clean signature of the dark matter annihilation.

In the Galactic center region, excesses of $\gamma$-rays were also reported by VERITAS [25] in the range above 2.8 TeV and by CANGAROO collaborations [26] in the range of 250 GeV to 1 TeV. Such excesses are also hard to be explained by conventional dark matter candidates. The HESS Collaboration also had a measurement of TeV gamma rays from the Galactic center [27], which is, to some extent, in disagreement with the CANGAROO results. It was pointed out [28] that this TeV $\gamma-$ray excess is likely to be of astrophysical origin and thus it constitutes a background for detecting dark matter annihilation. The origin of these backgrounds may be due to violent acceleration of cosmic protons and other particles by the chaotic magnetic fields near the Galactic center black hole [29]. After escaping the black hole environment and fly off into the interstellar medium, these extremely high energy protons collide with low energy protons (hydrogen gas) to form pions, which subsequently decay into high energy $\gamma$-rays that can radiate in all directions.

Due to its unknown astrophysical origin, it is hard to establish accurately the true continuum $\gamma$-ray background which could be used for comparison with dark matter annihilation. Thus, using the continuum $\gamma$-ray signal is difficult to provide strong evidence for



JHEP03(2007)120

dark matter, unless the dark matter annihilation rate is very large. On the other hand, provided that the annihilation cross section is sufficiently large, the monochromatic photon line would be a "smoking gun" signal for dark matter annihilation, since the energy of the $\gamma$-ray is uniquely determined by the mass of the milli-charged dark matter (and the $Z'$ mass as well in the $\chi\bar{\chi} \to \gamma Z'$ channel). Nevertheless, the EGRET and HESS continuum backgrounds still pose a serious challenge to detecting the monochromatic photon line due to dark matter annihilation in the Galactic center region [28]. It was shown in ref. [28] that in order for a photon line to be detected above the continuum background, the quantity $(\sigma v/10^{-29}\ \mathrm{cm}^3\,\mathrm{s}^{-1})\,\overline{J}\,\Delta\Omega$ must be larger than $10-100$. This implies that the photon flux to be larger than $1.9\times(\mathrm{TeV}/m_\chi)^2\times(10^{-14}-10^{-13})\ \mathrm{cm}^{-2}\ \mathrm{s}^{-1}$. From figure 2, it is easy to see that for $m_\chi$ between 150 and 300 GeV, the photon flux in the $\chi\bar{\chi} \to \gamma Z'$ channel is close to the detectability level.

One may also give a rough estimate for continuum photon flux arises from the milli-charged dark matter annihilation into light quark pairs. The continuum photon spectrum mainly comes from the light quark fragmentation into neutral pions, which subsequently decay into secondary photons. The differential spectrum $dN_\gamma/dE_\gamma$ can be obtained by Monte Carlo event generators, e.g. PYTHIA, and then parameterized as a quark fragmentation function. We can use eq. (3.7) with $dN_\gamma/dE_\gamma$ given by a fragmentation-like function [30]:

$$\frac{dN_\gamma}{dx} = \eta\, x^a \exp(b + cx + dx^2 + ex^3)\ , \tag{3.10}$$

where $x = E_\gamma/m_\chi$ and for a light quark, e.g. $u$ or $d$ quark at an energy of 500 GeV, $\eta = 1$, $a = -1.5$, $b = 0.047$, $c = -8.7$, $d = 9.14$, and $e = -10.3$. These coefficients depend only mildly on the energy of the light quarks [30]. Putting all these factors together, we estimate the integrated photon flux with $E_\gamma > 1$ GeV to be of the order of $10^{-10}$ ($10^{-11}$) $\mathrm{cm}^{-2}\ \mathrm{s}^{-1}$ for $m_\chi = 100$ (500) GeV. It is at most around or slightly below the sensitivity level of GLAST. Since the VERITAS and HESS experiments are sensitive to higher energy and the above spectrum eq. (3.10) falls off rapidly as $x$ increases, their integrated photon fluxes are at least an order of magnitude smaller than that of GLAST. Despite challenging by the uncertain astrophysical backgrounds, this continuous secondary photon spectrum together with the monochromatic photon line from milli-charged dark matter annihilation can be probed by the next generation of $\gamma$-ray experiments.

## 4. Collider phenomenology

Phenomenology of the Stueckelberg $Z'$ with the presence of the hidden fermion-antifermion $\chi$ and $\bar{\chi}$ that the $Z'$ can decay into is quite different from the one studied before in refs. [1, 2].

The partial width of $Z'$ into a SM fermion pair $f\bar{f}$ is given by

$$\Gamma(Z' \to f\bar{f}) = \frac{N_f \beta_f}{24\pi} m_{Z'} \left[ \left( {\epsilon^{f_L}_{Z'}}^2 + {\epsilon^{f_R}_{Z'}}^2 \right) \left( 1 - \frac{m_f^2}{m_{Z'}^2} \right) + 6\, \epsilon^{f_L}_{Z'}\, \epsilon^{f_R}_{Z'} \frac{m_f^2}{m_{Z'}^2} \right] \tag{4.1}$$

and into hidden fermion pair $\chi\bar{\chi}$ is simply

$$\Gamma(Z' \to \chi\bar{\chi}) = \frac{\beta_\chi}{12\pi} m_{Z'} {\epsilon^{\chi}_{Z'}}^2 \left( 1 + \frac{2\, m_\chi^2}{m_{Z'}^2} \right)\ . \tag{4.2}$$

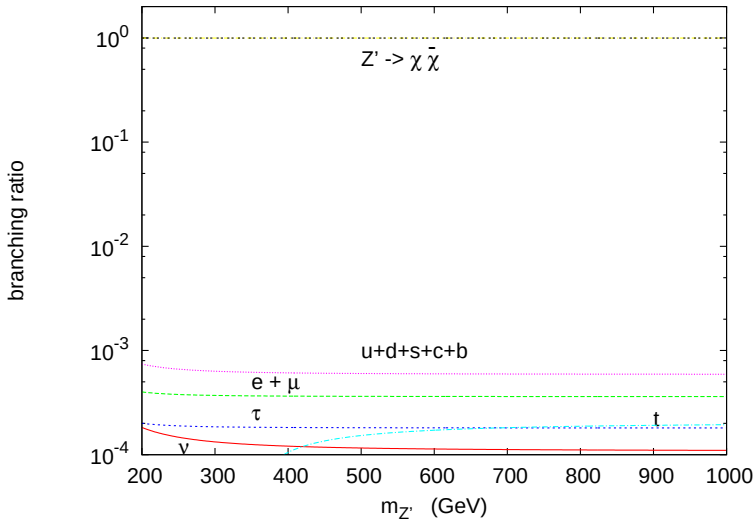


**Figure 3:** Branching ratios for $Z'$ with $g_X = g_2$, $\delta = 0.03$, and $m_\chi = 60$ GeV.

Here, $\beta_{f,\chi} = (1 - 4m_{f,\chi}^2/m_{Z'}^2)^{1/2}$. The total width of $Z'$ is evaluated by summing over all partial widths, including both the SM modes and the hidden mode. We show in figure 3 the various branching ratios for $Z'$ as a function of its mass with the following inputs $g_X = g_2$, $\delta = 0.03$, and $m_\chi = 60$ GeV. Since the mixing angle is so small ($\delta = 0.03$), the $Z'$ is mainly composed of the $C_\mu$ boson of the hidden sector. Hence, the $Z'$ dominantly decays into the hidden sector fermion pair while it has only a small fraction of $10^{-3}$ into visible fermions. The strategy for the search of this $Z'$ would be very different from all the previous conventional $Z'$ models including the hidden Stueckelberg $Z'$ studied in [1, 2].

Before we explore for the possible collider phenomenology of the Stueckelberg $Z'$ boson and the hidden sector fermion $\chi$, we have to make sure that the new particles and the hidden sector interactions will not upset the existing data.

### 4.1 Constraints from invisible decays of $Z$ and quarkonia

Firstly, the SM $Z$ boson that is observed at LEP would decay into a pair of hidden fermions $\chi\bar{\chi}$, giving rise to additional invisible width other than the neutrinos. Because of the mixings among the three neutral gauge bosons, the $Z$ boson can couple to the $\chi\bar{\chi}$ pair via the mixing angle $s_\phi$. We have calculated the partial width of $Z \to \chi\bar{\chi}$ for $g_X = g_2$, $\delta = 0.03$ (consistent with the dark matter requirement), and $m_\chi = 0 - 45$ GeV. The partial width is about 0.24 MeV, which is much smaller than the uncertainty 1.5 MeV of the invisible width of the $Z$ boson [3]. Even if we allow a larger mixing angle $\delta = 0.061$ (its maximum value allowed by eq. (2.13)), the invisible width of $Z$ would be at most 1 MeV, which is still within the $1\sigma$ uncertainty of the data. If the mass of $\chi$ is beyond half of the $Z$ boson mass, the invisible width of the $Z$ boson would not constrain the model.

The hidden fermion $\chi$ can also couple to the photon via the mixing angles $c_\theta s_\phi$, the maximum of which is about $0.9 \times 0.03 \approx 0.03$. Therefore, effectively the fermion $\chi$ "acquires" an electric charge of $g_X Q_X^\chi c_\theta s_\phi / e \approx 0.06$ when its coupling to the photon is con-



JHEP03(2007)120

sidered. If $\chi$ is very light, of the order of MeV, it could be produced in $J/\psi$ and $\Upsilon$ decays as invisible particles. Constraints on invisible decays of $J/\psi$ and $\Upsilon$ exist (for a comprehensive review on constraints on light dark matter: see ref. [31]). A very recent update on the $\Upsilon(1S)$ invisible width is given in ref. [32]. The invisible widths of $J/\psi$ and $\Upsilon$ are respectively

$$B(J/\psi \to \text{invisible}) < 7 \times 10^{-3} \quad \text{and} \quad B(\Upsilon(1S) \to \text{invisible}) < 2.5 \times 10^{-3} \,.$$

However, the partial width of $J/\psi$ into $\chi\bar{\chi}$ is suppressed by the milli-charged factor of $(0.06)^2$ relative to the partial width into $e^-e^+$. Thus $B(J/\psi \to \chi\bar{\chi}) \approx (0.06)^2 \times B(J/\psi \to e^-e^+) \approx 10^{-4}$, which is well below the above limit. The situation for $\Upsilon$ invisible decay is very similar: $B(\Upsilon(1S) \to \chi\bar{\chi}) \approx (0.06)^2 \times B(\Upsilon(1S) \to e^-e^+) \approx 10^{-4}$, which is also safe. Indeed, a recent study [33] using $400\,\text{fb}^{-1}$ luminosity collected at the $\Upsilon(4S)$, the B-factory can limit $B(\Upsilon(1S) \to \text{invisible}) \lesssim 10^{-3}$. There are also other decays modes, such as $J/\psi$ or $\Upsilon \to \gamma + \text{invisible}$, but it is straightforward to check that with an effective charge of 0.06 the experimental limits of these radiative invisible modes do not constrain the model at all. If the mass $m_\chi$ is above 5 GeV, it has no constraint at all from these invisible decays of the quarkonia.

### 4.2 Constraint from singly production of $Z'$ at LEPII

Singly production of the $Z'$ at LEPII is possible via $e^-e^+ \to \gamma Z'$ followed by the invisible decay of the $Z'$. This process is very similar to the SM process $e^-e^+ \to \gamma Z \to \gamma\nu\bar{\nu}$. The differential cross section for $e^-e^+ \to \gamma Z'$ is given by

$$\frac{d\sigma(e^-e^+ \to \gamma Z')}{d\cos\Theta} = \frac{\beta_{Z'} e^2 Q_e^2}{32\pi s} \left(\epsilon_{Z'}^{e_L\,2} + \epsilon_{Z'}^{e_R\,2}\right) \frac{1}{ut} \left[t^2 + u^2 + 2sm_{Z'}^2\right] \,, \tag{4.3}$$

where $\Theta$ is the scattering angle of the photon, $t = -s\beta_{Z'}(1 - \cos\Theta)/2$, $u = -s\beta_{Z'}(1 + \cos\Theta)/2$, and $\beta_{Z'} = (1 - m_{Z'}^2/s)$. We show the production cross section at LEPII energy $\sqrt{s} = 205$ GeV in figure 4 as a function of $m_{Z'}$. Since the $Z'$ would decay into invisible $\chi\bar{\chi}$, the signal of which would be a mono-photon. The recoil mass spectrum would then indicate the mass of the $Z'$. In the figure, we also show the 95% C.L. upper limits on mono-photon production as a function of the missing mass obtained by DELPHI [34]. A small mass range of $Z'$, 180 GeV $\lesssim m_{Z'} \lesssim$ 200 GeV, is disfavored by the data. However, one has to be cautious in this relatively soft photon region where large theoretical uncertainties are expected to be important.

### 4.3 Drell-Yan production of $Z'$ at the Tevatron

The production cross section of $Z'$ followed by the leptonic decay at the Tevatron is given by

$$\sigma(p\bar{p} \to Z' \to \ell^-\ell^+) = \frac{1}{144}\frac{1}{s}\frac{m_{Z'}}{\Gamma_{Z'}} \left(\epsilon_{Z'}^{\ell_L\,2} + \epsilon_{Z'}^{\ell_R\,2}\right) \sum_{q=u,d,s,c} \left(\epsilon_{Z'}^{q_L\,2} + \epsilon_{Z'}^{q_R\,2}\right) \int_r^1 \frac{dx}{x} f_q(x)\, f_{\bar{q}}\left(\frac{r}{x}\right) \tag{4.4}$$

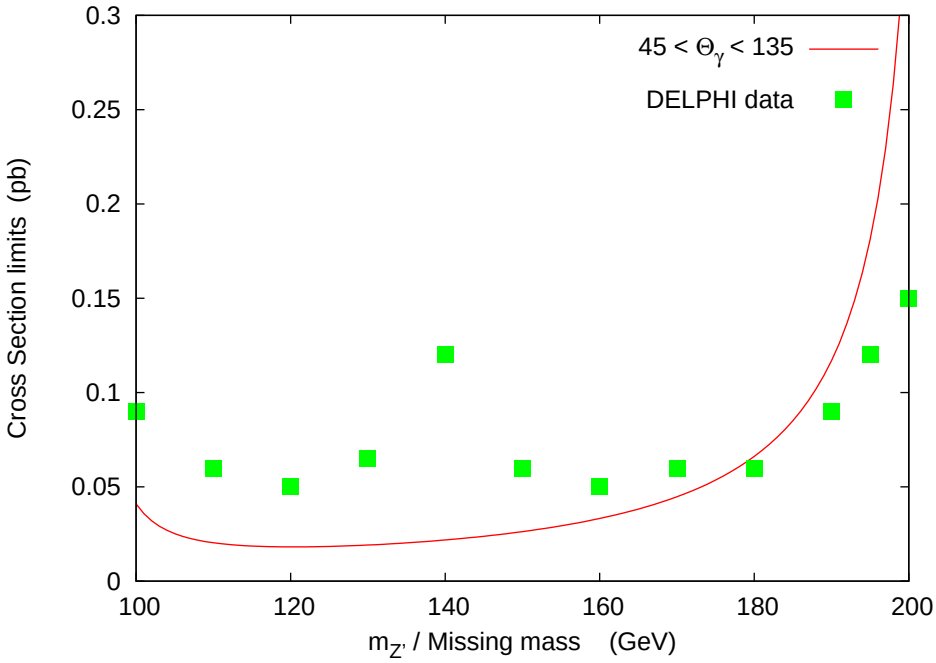


**Figure 4:** Comparison with the DELPHI data on the mono-photon production. The theory prediction is for $g_X = g_2$ and $\delta = 0.03$.

where $\sqrt{s} = 1960$ GeV, $r = m_{Z'}^2/s$, $\Gamma_{Z'}$ is the total width of $Z'$ given in eqs. (4.1) and (4.2), and $\epsilon_{Z'}^{f_{L,R}}$ can be found in eq. (2.12). This Drell-Yan cross section for the $Z'$ boson is plotted in figure 5, where the 95% C.L. upper limits on $\sigma(Z') \cdot B(Z' \to e^- e^+)$ from the CDF preliminary results [35] are also shown. It is clear that the present CDF limits do not constrain the model at all. This is in sharp contrast to the results studied in ref. [2] because the $Z'$ boson that we consider here has a very small branching fraction into charged lepton pair. The $Z'$ boson would decay preferably into the hidden sector fermions instead of visible particles. On the other hand, the Stueckelberg $Z'$ in ref. [2] only decays into the SM particles. In our case the $Z'$ only has a branching ratio of $\sim 10^{-4} - 10^{-3}$ into leptonic pairs, and it would not be easily detected in the Drell-Yan channel. Neither the hadronic decay modes of $Z'$ can afford it to be detected. Even in the future runs of the Tevatron with a sensitivity reaching the level of $10^{-3} - 10^{-2}$ pb, it is still not possible to detect this kind of $Z'$ boson through the Drell-Yan channel.

### 4.4 Singly production of $Z'$ at LHC and ILC

Perhaps one has to rely on the invisible decay mode of the Stueckelberg $Z'$ of this model to identify its presence. Here we calculate the predictions of singly $Z'$ production at the LHC and ILC. Other than the Drell-Yan process that we have considered, the next relevant process to probe this invisible $Z'$ is via $q\bar{q} \to gZ'$ followed by $Z' \to \chi\bar{\chi}$, which gives rise to monojet events. The subprocess cross section can be easily adapted from eq. (4.3):

$$\frac{d\hat{\sigma}(q\bar{q} \to gZ')}{d\cos\theta^*} = \frac{\beta_{Z'} g_s^2}{72\pi\hat{s}} \left(\epsilon_{Z'}^{q_L 2} + \epsilon_{Z'}^{q_R 2}\right) \frac{1}{\hat{u}\,\hat{t}} \left[\hat{t}^2 + \hat{u}^2 + 2\,\hat{s}\,m_{Z'}^2\right] . \tag{4.5}$$

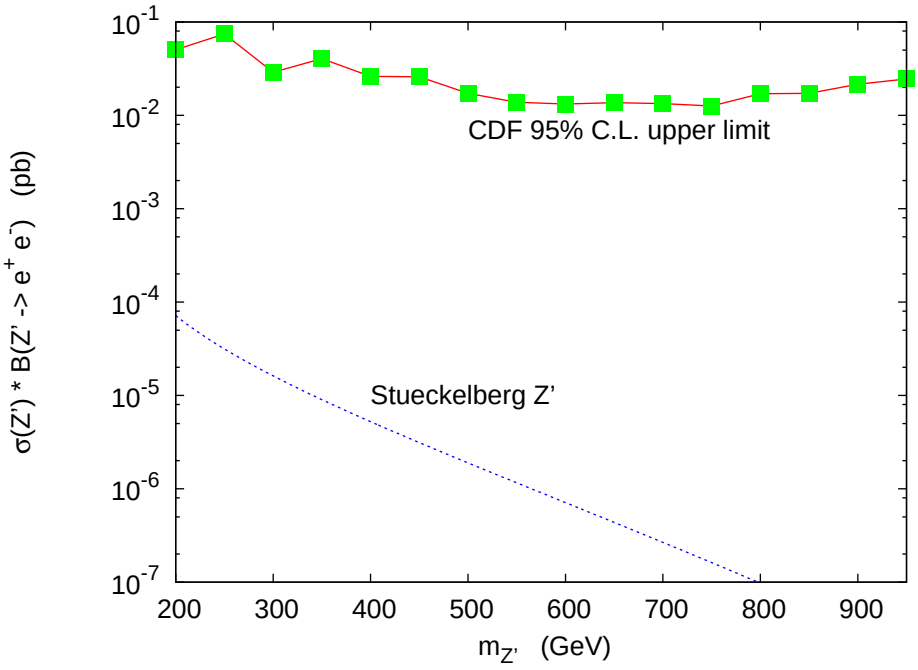


**Figure 5:** Drell-Yan cross sections $p\bar{p} \to Z' \to e^-e^+$ versus $m_{Z'}$ for $g_X = g_2$ and $\delta = 0.03$. We also show the 95% C.L. upper limits on $\sigma(Z') \cdot B(Z' \to e^-e^+)$ from the CDF preliminary results [35].

Other cross channels, e.g., $qg \to qZ'$, can be obtained from eq. (4.5) using the crossing symmetry. The branching ratio $B(Z' \to \chi\bar{\chi})$ is very close to unity. We show in figure 6 the production rate of monojet events versus $m_{Z'}$ with $g_X = g_2$ and $\delta = 0.03$ at the LHC under the jet cuts of $p_{Tj} > 20$ GeV and $|\eta_j| < 2.5$. The $q\bar{q}Z'$ coupling is suppressed by the small mixing angle, the same as in the Drell-Yan process, but unlike the Drell-Yan process, this monojet amplitude is suppressed by only one power of the mixing angle instead of two. Therefore, the rate is not negligible. Also, the true SM background for monojet is rather rare. Thus, the monojet event actually signals the presence of such an invisible $Z'$.

Another place to detect such an invisible $Z'$ is at the ILC with the process $e^-e^+ \to \gamma Z' \to \gamma\chi\bar{\chi}$, which we have considered above for the mono-photon limits from LEP. We extend the energy to $0.5 - 1.5$ TeV and calculate the event rates for the mono-photon final state. We show in figure 7 the production rates at $\sqrt{s} = 0.5, 1, 1.5$ TeV with $g_X = g_2$ and $\delta = 0.03$.

## 5. Conclusions

We have proposed an extension of the Stueckelberg $Z'$ standard model by adding a pair of fermion and antifermion in the hidden sector, which has only a $U(1)_X$ symmetry. The stability of the hidden fermion pair with its weak sized interaction makes it a suitable dark matter candidate with a correct amount of dark matter density. We have calculated the photon flux from the Galactic center due to the annihilation of this milli-charged dark matter. If $2m_\chi < m_{Z'}$, there is only a small range of $m_\chi$ that the photon flux is above the



JHEP03(2007)120

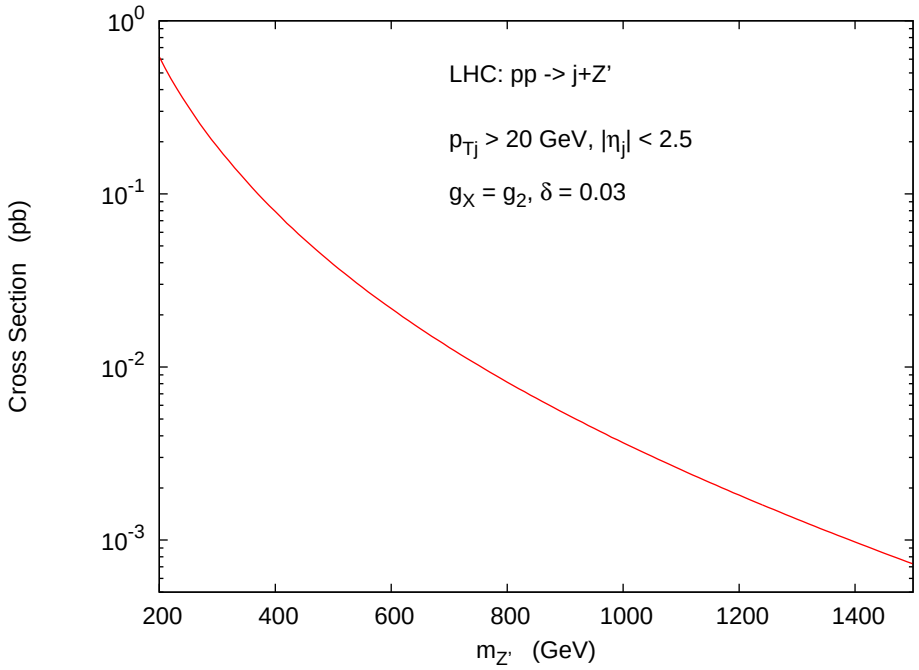


**Figure 6:** Production cross section for the process $pp \to j + Z'$ followed by invisible decay of the $Z'$ with $g_X = g_2$ and $\delta = 0.03$ at the LHC. We imposed $p_{Tj} > 20$ GeV and $|\eta_j| < 2.5$ on the jet.

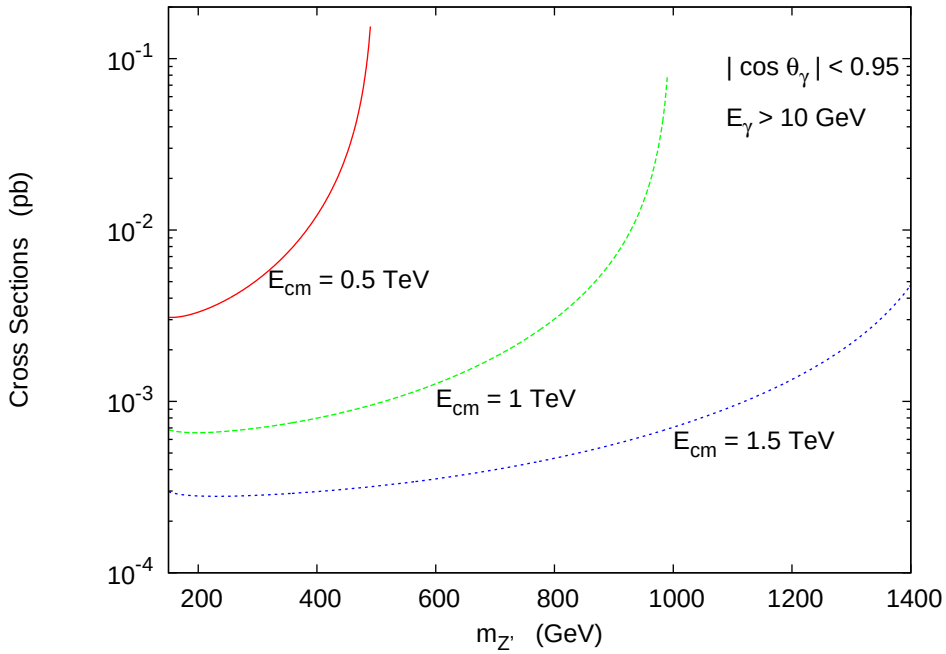


**Figure 7:** Production cross section for the process $e^- e^+ \to \gamma + Z'$ followed by invisible decay of the $Z'$ with $g_X = g_2$ and $\delta = 0.03$ at ILC ($\sqrt{s} = 0.5$, 1, 1.5 TeV). We imposed $E_\gamma > 10$ GeV and $|\cos_\gamma| < 0.95$ on the photon.

JHEP03(2007)120

sensitivity level of the future $\gamma$-ray experiments. However, if $2m_\chi > m_{Z'}$ there is a wide range of $m_\chi$ that the photon flux is above the sensitivity level. The collider phenomenology may be different from those studied in ref. [2], because the dominant decay of the $Z'$ is into the invisible $\chi\bar{\chi}$ if kinematically allowed. In this case, the present Drell-Yan data cannot constrain the model at all. We have proposed the monojet signal at the LHC and the mono-photon signal at the future ILC to probe this invisibly decaying Stueckelberg $Z'$ boson.

We close with some comments.

1. Since only a $U_X(1)$ symmetry is assumed in the hidden sector, each hidden fermion is stable against decay. Therefore, if we assume more fermion pairs in the hidden sector, their relic densities are additive. Thus, a larger coupling constant is needed to ensure larger annihilation cross sections. One can also consider multiple hidden Stueckelberg $U(1)$ extension of the SM. We refer to ref. [1] for the discussion for this possibility.

2. When $m_{Z'} < 2m_\chi$, the $Z'$ decays dominantly into visible particles. It can be easily detected in the Drell-Yan channel. The existing data constrains the model, as given by eq. (2.14) originally obtained by the authors in ref. [2]. Photon flux from pair annihilation of $\chi\bar{\chi} \to \gamma Z'$ at the Galactic center is also within reach at the next generation of $\gamma$-ray experiments.

3. When $m_{Z'} > 2m_\chi$, the $Z'$ decays dominantly into invisible $\chi\bar{\chi}$. The present Drell-Yan data cannot constrain the model, neither can the invisible decays of $J/\psi$ and $\Upsilon$ for a very light $\chi$. However, the mono-photon production limits obtained by DELPHI disfavors a small range of 180 GeV $\lesssim m_{Z'} \lesssim$ 200 GeV. We anticipate that in the future ILC the missing mass spectrum can efficiently constrain this type of invisibly decaying $Z'$ boson.

4. The hidden fermion appears to have a milli-charge as it acquires a small effective coupling to the photon through the mixing induced by the combined Higgs and Stueckelberg mechanisms. With a mass of $O(100)$ GeV and an effective charge 0.06 of a unit charge, the hidden fermions are consistent with the existing constraints on milli-charged particles [6]. As milli-charged particle is of very recent interests [12], an update on the terrestrial and astrophysical constraints on this hidden milli-charged particle is desirable.

## Acknowledgments

We would like to thank Pran Nath for encouragement and Holger Gies for useful comments on the manuscript. K.C. also thanks K.S. Cheng and the Centre of Theoretical and Computational Physics at the University of Hong Kong for hospitality. This research was supported in part by the National Science Council of Taiwan R.O.C. under Grant No. NSC 95-2112-M-007-001 and by the National Center for Theoretical Sciences.

**Note added.** Stueckelberg $Z'$ extension with kinetic mixing has been studied recently in [36]. Wherever overlaps in the parameter space, the authors in [36] found agreements with the analysis presented in our work.

## References


[1] B. Körs and P. Nath, *Aspects of the Stueckelberg extension*, *JHEP* **07** (2005) 069 [hep-ph/0503208]; *A Stueckelberg extension of the standard model*, *Phys. Lett.* **B 586** (2004) 366 [hep-ph/0402047].

[2] D. Feldman, Z. Liu and P. Nath, *Probing a very narrow Z' boson with cdf and d0 data*, *Phys. Rev. Lett.* **97** (2006) 021801 [hep-ph/0603039].

[3] W.M. Yao *et al.*, *Review of particle physics*, *J. Phys.* **G 33** (2006) 1.

[4] H. Goldberg and L.J. Hall, *A new candidate for dark matter*, *Phys. Lett.* **B 174** (1986) 151.

[5] B. Holdom, *Two U(1)'s and $\epsilon$ charge shifts*, *Phys. Lett.* **B 166** (1986) 196; *Searching for $\epsilon$ charges and a new U(1)*, *Phys. Lett.* **B 178** (1986) 65.

[6] S. Davidson, S. Hannestad and G. Raffelt, *Updated bounds on Milli-charged particles*, *JHEP* **05** (2000) 003 [hep-ph/0001179];
S. Davidson, B. Campbell and D.C. Bailey, *Limits on particles of small electric charge*, *Phys. Rev.* **D 43** (1991) 2314.

[7] A. Gould, B.T. Draine, R.W. Romani and S. Nussinov, *Neutron stars: graveyard of charged dark matter*, *Phys. Lett.* **B 238** (1990) 337.

[8] S.L. Dubovsky, D.S. Gorbunov and G.I. Rubtsov, *Narrowing the window for millicharged particles by CMB anisotropy*, *JETP Lett.* **79** (2004) 1 [hep-ph/0311189].

[9] A. De Rujula, S.L. Glashow and U. Sarid, *Charged dark matter*, *Nucl. Phys.* **B 333** (1990) 173.

[10] M.Y. Khlopov, *New symmetries in microphysics, new stable forms of matter around us*, astro-ph/0607048.

[11] PVLAS collaboration, E. Zavattini et al., *Experimental observation of optical rotation generated in vacuum by a magnetic field*, *Phys. Rev. Lett.* **96** (2006) 110406 [hep-ex/0507107].

[12] H. Gies, J. Jaeckel and A. Ringwald, *Polarized light propagating in a magnetic field as a probe of millicharged fermions*, *Phys. Rev. Lett.* **97** (2006) 140402 [hep-ph/0607118].

[13] S.-J. Chen, H.-H. Mei and W.-T. Ni, *Q & A experiment to search for vacuum dichroism, pseudoscalar-photon interaction and millicharged fermions*, hep-ex/0611050;
S.-J. Chen, H.-H. Mei, W.-T. Ni and J.-S. Wu, *Improving ellipticity detection sensitivity for the Q & A vacuum birefringence experiment*, hep-ex/0308071.

[14] M. Ahlers, H. Gies, J. Jaeckel and A. Ringwald, *On the particle interpretation of the PVLAS data: neutral versus charged particles*, *Phys. Rev.* **D 75** (2007) 035011 [hep-ph/0612098].

[15] G. Bertone, D. Hooper and J. Silk, *Particle dark matter: evidence, candidates and constraints*, *Phys. Rept.* **405** (2005) 279 [hep-ph/0404175].

[16] WMAP collaboration, D.N. Spergel et al., *Wilkinson microwave anisotropy probe (WMAP) three year results: implications for cosmology*, astro-ph/0603449.




JHEP03(2007)120

[17] P. Gondolo and J. Silk, *Dark matter annihilation at the galactic center*, *Phys. Rev. Lett.* **83** (1999) 1719 [astro-ph/9906391].

[18] L. Bergstrom and P. Ullio, *Full one-loop calculation of neutralino annihilation into two photons*, *Nucl. Phys.* **B 504** (1997) 27 [hep-ph/9706232].

[19] K. Cheung, C.-W. Chiang and J. Song, *A minimal supersymmetric scenario with only $\mu$ at the weak scale*, *JHEP* **04** (2006) 047 [hep-ph/0512192].

[20] K. Cheung and C.-W. Chiang, *Splitting the split supersymmetry*, *Phys. Rev.* **D 71** (2005) 095003 [hep-ph/0501265].

[21] The HESS collaboration, J.A. Hinton, *The status of the HESS project*, *New Astron. Rev.* **48** (2004) 331–337 [astro-ph/0403052].

[22] T.C. Weekes et al., *VERITAS: the very energetic radiation imaging telescope array system*, astro-ph/9706143.

[23] N. Gehrels and P. Michelson, *GLAST: The next generation high-energy gamma-ray astronomy mission*, *Astropart. Phys.* **11** (1999) 277.

[24] H. A. Mayer-Hasselwander *et al.*, *High-energy gamma ray emission from the galactic center*, *Astron. Astrophys.* **335** (1998) 161.

[25] The VERITAS collaboration, K. Kosack et al., *TeV gamma-ray observations of the galactic center*, *Astrophys. J.* **608** (2004) L97–L100 [astro-ph/0403422].

[26] CANGAROO-II collaboration, K. Tsuchiya et al., *Detection of sub-tev gamma-rays from the galactic center direction by CANGAROO-II*, *Astrophys. J.* **606** (2004) L115–L118 [astro-ph/0403592].

[27] The HESS collaboration, F. Aharonian et al., *Very high energy gamma rays from the direction of sagittarius A**, *Astron. Astrophys.* **425** (2004) L13–L17 [astro-ph/0408145].

[28] G. Zaharijas and D. Hooper, *Challenges in detecting gamma-rays from dark matter annihilations in the galactic center*, *Phys. Rev.* **D 73** (2006) 103501 [astro-ph/0603540].

[29] Information is available at http://uanews.org/cgi-bin/WebObjects/UANews.woa/4/wa/SRStoryDetails?ArticleID=13601.

[30] N. Fornengo, L. Pieri and S. Scopel, *Neutralino annihilation into gamma-rays in the milky way and in external galaxies*, *Phys. Rev.* **D 70** (2004) 103529 [hep-ph/0407342].

[31] P. Fayet, *Constraints on light dark matter and U bosons, from $\psi$, $\Upsilon$, $K^+$, $\pi^0$, $\eta$ and $\eta'$ decays*, *Phys. Rev.* **D 74** (2006) 054034 [hep-ph/0607318].

[32] Belle collaboration, O. Tajima et al., *Search for invisible decay of the $\Upsilon(1S)$*, hep-ex/0611041.

[33] B. McElrath, *Invisible quarkonium decays as a sensitive probe of dark matter*, *Phys. Rev.* **D 72** (2005) 103508 [hep-ph/0506151].

[34] DELPHI collaboration, J. Abdallah et al., *Photon events with missing energy in $e^+e^-$ collisions at $\sqrt{s}$ = 130-GeV to 209-GeV*, *Eur. Phys. J.* **C 38** (2005) 395 [hep-ex/0406019].

[35] Information is available at http://www-cdf.fnal.gov/∼harper/diEleAna.html.

[36] D. Feldman, Z. Liu and P. Nath, *The stueckelberg Z' extension with kinetic mixing and milli-charged dark matter from the hidden sector*, hep-ph/0702123.

JHEP03(2007)120